

Angular momentum distribution during the collapse of primordial star-forming clouds

Jayanta Dutta

Abstract It is generally believed that angular momentum is distributed during the gravitational collapse of the primordial star forming cloud. However, so far there has been little understanding of the exact details of the distribution. We use the modified version of the Gadget-2 code, a three-dimensional smoothed-particle hydrodynamics **simulation**, to follow the evolution of the collapsing gas in both idealized as well as more realistic minihalos. We find that, despite the lack of any initial turbulence and magnetic fields in the clouds the angular momentum profile follows the same characteristic power-law that has been reported in studies that employed fully self-consistent cosmological initial conditions. The fit of the power-law appears to be roughly constant regardless of the initial rotation of the cloud. We conclude that the specific angular momentum of the self-gravitating rotating gas in the primordial minihalos maintains a scaling relation with the gas mass as $L \propto M^{1.125}$. We also discuss the plausible mechanisms for the power-law distribution.

Keywords stars: formation – stars: early universe – hydrodynamics – instabilities

1 Introduction

The significant progress in the theoretical as well as numerical calculations **has provided a** great stride in our understanding of the history of the Universe, especially the transition period from the ‘Cosmic Dark Ages’ to

the first source of light to the present-day clumpy structure of the Universe (Madao 2000; Barkana & Loeb 2001; Heger & Woosley 2002; Umeda & Nomoto 2003; Schneider et al. 2003; Frebel et al. 2005). In last two decades, there have been extensive studies on the hierarchical structure formation that eventually leads to the collapse of the first gravitationally and thermally unstable primordial gas clouds (Reed et al. 2005; Ciardi & Ferrara 2005; Yoshida et al. 2006; O’Shea & Norman 2007). **It has been shown that the angular momentum of the dark matter (DM) and baryons become comparable during virialization (Wise & Abel 2007).** The physics that determines the collapse is extremely complex along with **a complicated** chemical network, and is intrinsically multidimensional, non-linear and **not in equilibrium** (Glover & Abel 2008; Whalen et al. 2008; Bromm et al. 2009; Hosokawa et al. 2011; Johnson et al. 2013).

One of the interesting physical problems is **the distribution of the angular momentum of the baryons that have collapsed gravitationally within minihalos (Larson 1969, 1972; Silk 1977; Norman et al. 1980; Couchman & Rees 1986).** This process ultimately leads to the formation and evolution of the very first stars in the Universe, the so-called Population III (or Pop III) stars (e.g. Haiman et al. 1996; Tegmark et al. 1997; Omukai & Nishi 1998). **Numerical computations using various methods (primarily Lagrangian and Eulerian code) make it possible to study the gas dynamics with higher spatial resolution** (e.g., Bromm Coppi & Larson 1999; Abel et al. 2000). These calculations conclude that the angular momentum of the continually collapsing core is just a fraction of the total angular momentum of the cloud in which the high-density core forms (Abel et al. 2002; Fisher 2004; Jappsen & Klessen 2004). Clearly angular momentum must be redistributed during the star for-

Jayanta Dutta

¹Instituto de Astrofísica e Ciências do Espaço, Universidade de Lisboa, OAL, Tapada da Ajuda, PT1349-018 Lisboa, Portugal

²Raman Research Institute, C. V. Raman Avenue, Sadashivanagar, Bengaluru, Karnataka 560080
jd.astrop@gmail.com

mation (O’Shea & Norman 2008; Yoshida et al. 2008; Turk et al. 2009).

The angular momentum in protogalaxies also has substantial effect on the temperature evolution (Vasiliev Vorobyov & Shchekinov 2010). They concluded that the increase of rotational angular momentum of the gas results in cooling of the gas to a temperature less than 100 K. It is therefore obvious that the existence of initial angular momentum can delay the formation of the primordial stars. Even the efficiency of fragmentation and the star formation rate in primordial gas becomes sensitive to the angular momentum (Bromm et al. 2002). The same conclusion has been drawn by Dutta et al. (2012) that shows that the cloud with higher angular momentum leads the gas to have a lower temperature compared to their slowly rotating counterparts. More recently, the angular speed of the first stars has been investigated thoroughly using the sink particles method (a computational technique in which a certain high density regime is considered as a growing protostars that can accrete gas particles) in cosmological simulations by Stacy et al. (2011). Although angular momentum is conserved during the collapse of a rotating gaseous cloud, a small fraction of the cloud’s mass at the center can collapse to stellar densities, leaving behind the rest of cloud in an extended rotationally supported envelope that fragments (Clark et al. 2011). The fraction of the collapsing cloud that ends up in a star or stellar system depends on the amount of angular momentum transferred outward during the collapse (e.g., Greif et al. 2012; Stacy & Bromm 2013).

The recent simulations, e.g., using the moving mesh code *Arepo* by Greif (2015) and using smoothed particle hydrodynamics (SPH) by Dutta (2015b) have addressed the important issues such as transfer and redistribution of the angular momentum while describing the velocity structure, accretion and thermal evolution of gas in a number of mini-halos. The analytic models for the rapidly rotating disks in the presence of turbulence and UV backgrounds have been discussed in a series of papers (Latif et al. 2015, and references therein). In addition, there is strong indication of the dependency of the angular momentum on the Pop III accretion rate in the current literature (Hirano et al. 2015). However, so far there has been little understanding on the **basic characteristic** of cloud’s angular momentum distribution and its evolution during the gravitational collapse of the primordial star forming gas. The extent to which the angular momentum of the cloud depends on the initial strength of rotation has never been systematically

tested. **Moreover, there is still ambiguity of the basic physical mechanism that is responsible for the distribution of angular momentum in primordial clouds.** In our recent study, we have **taken care to address** the influence of the initial rotation of the primordial cloud on the thermal, chemical and dynamical evolution that results in the fragmentation of the disk (Dutta 2015b). In this work, we revisit the physics of gravitational collapse of the primordial gas with a particular focus on the angular momentum profile in the evolutionary stage. Our approach to investigate the gas evolution is different from the previous studies in the sense that we **scrutinize** the angular momentum distribution for a large set of simulations with a varied initial degree of rotation of the gas clump **and compare the result with more realistic cosmological simulations that was based on different numerical formalism.** We have studied the gas collapse till it attains the protostellar densities.

In the next section §2, we briefly outline the numerical set-up of simulations and initial conditions. We then discuss the relevant physical concept of the problem with an emphasis on the origin and distribution of the angular momentum of the collapsing gas in §3. We draw our conclusions in §4.

2 Simulations

To investigate the angular momentum distribution, we use a simple and straightforward numerical set-up where the gravitationally unstable gas clump is assumed to be spherical of size ~ 2.7 pc. For simplicity, we assume that gas particles are uniformly distributed with an initial number density $n_0 = 10^3 \text{ cm}^{-3}$ and temperature $T_0 = 200$ K. These values are consistent with the primordial gas cloud at redshift $z \geq 20$ (Abel et al. 2002; Bromm & Larson 2004).

Initially the gas clump contains only atomic hydrogen that will collapse only if the gravitational potential energy of the cloud is greater than the net kinetic energy. With no external source of cooling, the above criteria is fulfilled because the free-fall time ($t_{\text{ff}} = \sqrt{3\pi/32G\rho} = 1.37$ Myr) is shorter than the sound-crossing time $t_{\text{sc}} \approx 5$ Myr. The gas cloud therefore inevitably starts to collapse under the self-gravity. We use 5 million SPH particles to model the gas distribution in the cloud of total mass of $M \sim 3000 M_{\odot}$. The numerical resolution (for 100 SPH particles) is $0.06 M_{\odot}$.

With this set-up, the artificial clump is given initial angular momentum that can be obtained from the rotational (E_{rot}) and the gravitational (E_{grav}) energies of

gas particles. We follow Sterzik et al. (2003) to model the angular velocity of the cloud in which the decisive parameter β_0 , where $\beta_0 = E_{\text{rot}}/E_{\text{grav}} = R_0^3 \Omega_0^2 / 3GM_0$, sets the strength of rotational support of the gas clump. Here R_0 and Ω_0 are the radius and angular velocity of the gas clump. We perform six numerical experiments with varied β_0 parameters, whose magnitude spans two orders of magnitude.

We take care to ensure that our investigation is not biased by the artificial configuration of the gas clump. Hence we investigate the angular momentum distribution in two different minihalos (CH1 and CH2 of Dutta et al. 2015) obtained from cosmological simulations of the hydrodynamic moving mesh code *Arepo* (Springel 2010). We implement these realistic minihalos in our modified SPH Gadget-2 code (Springel 2005). We here mention that although both the codes, i.e., *Arepo* and Gadget-2 use different approach in solving hydrodynamics equations, both of them basically follow the Lagrangian formalism. This enables us to use the minihalos from the unstructured moving mesh into SPH configuration.

We summarise here the detailed configuration and initial conditions of these minihalos (see table 1 of Dutta 2015b for the detailed configuration of the halos). The gas density of both minihalos increases towards the centre of cloud and has a maximum value $n \sim 10^6 \text{ cm}^{-3}$. We have chosen this limit because the gas will go through a rapid phase of transition at density $n \geq 10^6 \text{ cm}^{-3}$ via three-body H_2 formation reaction (Palla et al. 1983)



We can therefore simulate the crucial transformation of the atomic to molecular hydrogen as the collapse proceeds to higher density. The rapid formation of the molecular hydrogen cools the gas very efficiently and initiate chemothermal instability (Dutta 2015a). Although the rate coefficient for this reaction is highly uncertain, we choose the intermediate one that is $7.7 \times 10^{-31} T^{-0.464} \text{ cm}^6 \text{ s}^{-1}$ (Glover 2008). The CH1 and CH2 contains gas mass of $1030 M_\odot$ and $1093 M_\odot$ respectively. The temperature at the center of both minihalos has a maximum value $\sim 450\text{K}$, while at the periphery it is around 50K . With altogether six million SPH particles in each of our simulations, we are able to resolve the angular velocity of

the gas significantly better than in the SPH models of our previous study. The numerical resolution of our simulations for both minihalos are of the order of $0.01 M_\odot$. **The initial rotation of minihalos, defined by the spin parameter (β_0), is 0.035 (for CH1) and 0.042 (for CH2) respectively. So the realistic minihalos falls intermediate compared to the idealized gas clump where we simulate the gravitational collapse of solid body with $\beta_0 = 0.0, 0.005, 0.01, 0.05, 0.1$ and 0.2 respectively.**

The chemical network for primordial collapse is extremely complex with primordial hydrogen, helium and deuterium mixing in a different way to contribute toward the thermal, chemical and dynamical evolution of gas. We follow Dutta et al. (2015) to model the time-dependent chemical reactions in this study. We use the modified version of the Gadget-2 momentum equation from our previous study Dutta (2015b) to model external pressure boundary for both the idealized as well as realistic minihalos.

3 Angular Momentum

It is a common feature of all star formation calculations that the angular momentum of a single star or star-cluster is much lower than that of the original cloud in which the protostars form (e.g. Bodenheimer 1995). We follow the collapse of primordial gas and study the distribution of the angular momentum for different degrees of initial rotation (β_0).

Fig. 1 shows the physical conditions in the gas once the central region has collapsed to a density of $\sim 5 \times 10^{13} \text{ cm}^{-3}$. The panels show mass-weighted averages of the properties of individual SPH particles within radial logarithmic bins. We find in Fig. 1A that regardless of the initial rotation speed, all clouds closely follow a power-law density profile $n \propto r^{-2.2}$, implying to a relation between the radius and enclosed mass $M \propto r^{4/5}$ (Fig. 1B). However, these are only approximate relations and different degrees of the rotationally support clouds lead to subtle deviations. For example, larger rotational support leads to a slightly steeper density gradient in the inner 10^4 AU , so that the enclosed mass within a certain radius is larger for the clouds with smaller β_0 values.

We plot the final and initial specific angular momentum profiles (i.e., angular momentum per unit mass shell) in Fig. 1C as a function of the enclosed gas mass. The solid lines represent the cloud's initial specific angular momentum (L_0), while the dot-dashed lines describe the final state. We see that the specific angular

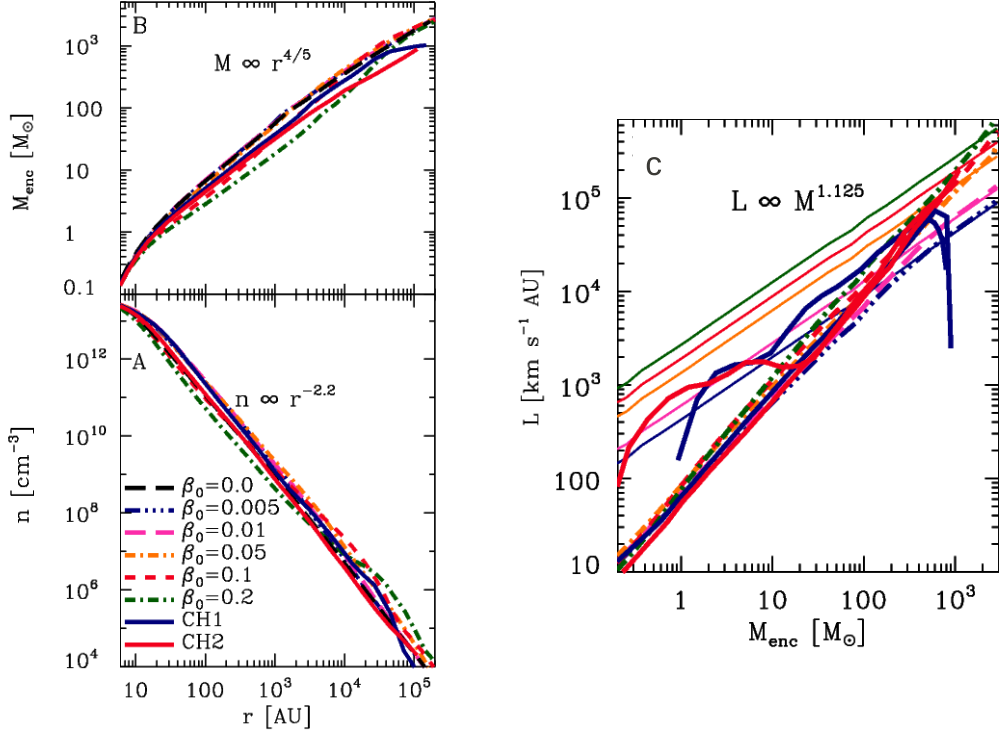


Fig. 1 (A) Radial logarithmic binned, mass-weighted averages of the number density (n) and (B) enclosed gas mass within the radius (r) are plotted as a function of the radius for different degrees of initial rotation of the cloud (β_0), including for the non-rotating case ($\beta_0 = 0$). These plots are created just before the formation of the first protostar. The specific angular momentum follows a power-law relation with the enclosed gas mass irrespective of the cloud's initial configuration. The solid lines represent the initial state of the angular momentum (L_0) for the different β_0 -modeled.

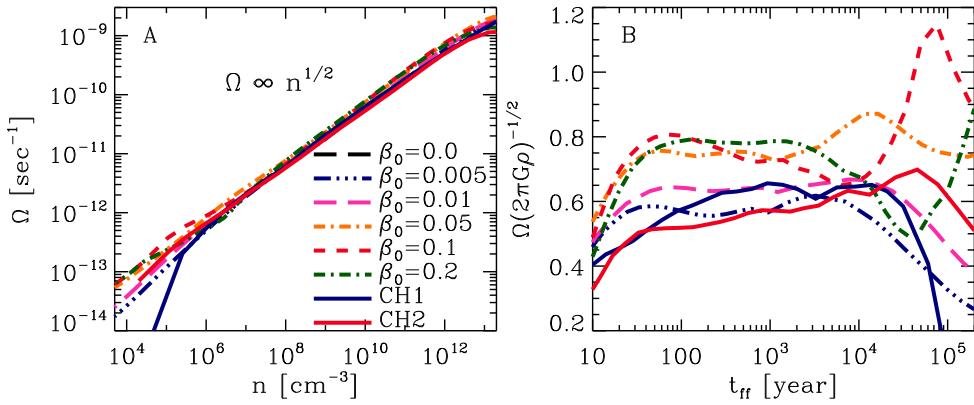


Fig. 2 (A) Radially binned, mass-weighted averages of the angular velocity is plotted as a function of the number density ($\Omega \propto n^{1/2}$) for different degrees of initial rotation (β_0). (B) Toomre's Q-parameter (defined as $Q = \Omega\sqrt{2\pi G\rho}$ (Matsumoto et al. 1997)) is nearly constant with the local free-fall time.

momentum changes significantly, resulting in its redistribution during the gravitational contraction. For the final state, we find that $L \propto M^{1.125}$ irrespective of the initial rotation of the cloud. We also note in Fig. 1A that it is the $\beta_0 = 0.2$ case that has the lowest values of n within the enclosed $10^3 M_\odot$ and the highest values of n outside this range at the evolutionary phase recorded here. That means cloud with $\beta_0 = 0.2$ has gone through an efficient phase of angular momentum distribution from the center to the periphery during the initial contraction.

This characteristic power-law behaviour has been reported in several studies (e.g., Abel et al. 2002; Yoshida et al. 2006; Clark et al. 2011) using cosmological initial conditions that are very different from our idealized initial conditions. We find the scaling relations of the characteristic angular momentum profile in two completely different gas distribution: (1) in idealized minihalos of five different simulations (with β_0 -model) and (2) in two realistic cosmological simulations. This rigorous **experiment suggests** that the power-law angular momentum distribution is a natural outcome of the collapsing gas, and may be a fundamental and universal property of the gravitational collapse of the primordial star-formation cloud.

3.1 Origin of the power-law slope

Hydrodynamical calculations of the gravitational collapse (e.g. Omukai & Nishi 1998) have shown that all clouds converge towards a higher-density regime that roughly obeys the power-law relation $n \propto r^{-2.2}$. We find that the non-rotating clouds ($\beta_0 = 0$) also have the similar density profile like their rotating counterparts. Previous studies have shown that the collapse approaches a self-similar solution, well-known for the non-rotating case (Larson 1969). Even for rotating clouds, it appears that the collapse still proceeds in a self-similar fashion (Matsumoto et al. 1997). From a dimensional analysis, one has $\Omega/\sqrt{G\rho} = \text{constant}$, where Ω is the angular velocity of the rotating cloud. Hence we have $\Omega \propto n^{1/2} \propto R^{-1.1}$ (Fig. 2A), followed by $\Omega \propto M^{-1.375}$. This leads to the angular momentum profile of the collapsed gas:

$$\boxed{L \propto \Omega r^2 \propto M^{1.125}}. \quad (3)$$

The relation in Fig. 2A is also satisfied for a homogeneous cloud in centrifugal equilibrium. Even in that case, $\Omega_K = v_K/r = \sqrt{GM}/r^3 \simeq \sqrt{G\rho(r)}$ for a mean density $\rho(r)$ within the radius r , where Ω_K is the angular velocity for Keplerian rotation. In Fig. 2B, we show the Toomre Q-parameter defined as $Q = \Omega/\sqrt{2\pi G\rho}$ (Matsumoto et al. 1997) plotted as a function of the

free-fall time. As expected, the quantity $\Omega(2\pi G\rho)^{-1/2}$ is roughly constant with the free-fall time of the collapsed gas. We conclude that the angular velocity and the angular momentum follow a pivotal power-law **relation** with the enclosed mass and are independent of the initial rotation and turbulence of the cloud. At this point, we also note that the specific angular momentum for the final state of the collapse does not necessarily depend on the initial density configuration. As the collapse proceeds to protostellar densities, one can always obtain the power-law angular momentum profile for both the initial uniform density and centrally condensed distribution.

3.2 Discussion on angular momentum distribution

As the gas continues to collapse, the angular momentum is continually distributed to maintain the angular velocities that are significant fraction of the Keplerian velocities. Unlike the present-day star formation where the rotation rate is reduced by the magnetized stellar winds and magnetic braking (Matt et al. 2010), the process of transferring the angular momentum during the primordial collapse is ambiguous and of utmost interest. Since the initial strength of rotation of the clouds can significantly affect the thermal as well as dynamical evolution of gas, a higher angular momentum **of** clouds can have different properties than their slowly rotating counterparts (Hirano et al. 2014; Dutta 2015b).

We adopt a Lagrangian point of view to calculate the time derivative of the specific angular momentum ($\tau = dL/dt$) for different mass shells that are logarithmic binned mass-weighted averages of SPH particles. **Following Yoshida et al. (2006)**, we can write the expression for two kinds of torques in the case of primordial gas collapse,

$$\begin{aligned} \frac{dL}{dt} &= \frac{d}{dt} \sum_{i=1}^n (\vec{r}_i \times \vec{v}_i) \\ &= \sum_{i=1}^n \vec{r}_i \times (\vec{F}_{\text{grav}} + \vec{F}_{\text{pres}}) \\ &= \vec{\tau}_{\text{grav}} + \vec{\tau}_{\text{pres}} \end{aligned} \quad (4)$$

where \vec{F}_{grav} is the total acceleration due to gravity, i.e., summation over all mass shell i , and \vec{F}_{pres} is the total force per unit mass due to the pressure gradients between the mass shells. We can therefore write the gravitational torques (τ_{grav}) and pressure torque (τ_{pres}) as following:

$$\begin{aligned}\vec{\tau}_{\text{grav}} &= \sum_{i=1}^n \vec{r}_i \times \frac{d\vec{v}_i}{dt} \\ \vec{\tau}_{\text{pres}} &= \sum_{i=1}^n \vec{r}_i \times \frac{\nabla P_i}{\rho_i}\end{aligned}\quad (5)$$

where \vec{r}_i is the distance of the mass shell i from the center, $d\vec{v}_i/dt$ is the acceleration due to gravity of the i^{th} shell, ρ_i is the density and ∇P_i is the pressure gradient between the shells. The sum goes over all SPH particles in spherical mass shell under consideration.

The gravitational torque is generated due to the nonaxisymmetric nature of the collapsing cloud or due to the spiral structure, which is consistent with the findings of previous studies (e.g., Yoshida et al. 2008; Lin et al. 2011). **For a rotating collapsing core, the non-radial gravitational forces due to the irregularities in the structure can produce a trailing spiral features of large amplitude (Larson 1984).** The associated gravitational torques can then transfer angular momentum outward on an orbital timescale. In the case of a clustered formation, the angular momentum could be efficiently transported outward by tidal torques, similar to the case of present-day star formation in a clustered environment (Bate et al. 2003). **Gravitational torques associated with gravitational instabilities also become important for angular momentum transport and energy dissipation in a self-gravitating accretion disk within a local viscous framework (Lodato & Rice 2004).** However, for a rotating collapsing core we find that the density gradient between the shells can produce the non-radial pressure torque. The concept of transferring angular momentum due to the pressure torque may be equivalent with the transport of angular momentum via hydrodynamic shocks during the turbulent collapse (as discussed in Abel et al. 2002).

For all β_0 modeled, we take into account both kind of forces in our simulations: one is the acceleration due to gravity that leads to the gravitational torque (τ_{grav}) and another is the pressure-torque (τ_{pres}). Here we refer the study by Larson (1984) that concluded that the non-axisymmetric nature of the cloud or inhomogeneities tend to form a spiral structure that produces the gravitational torque. The pressure forces can arise from the density gradient between the mass shells. We have observed that the gravitational and pressure torque act in opposite direction, though not always, and change direction throughout the collapsing gas cloud. However, the contribution of the torques will

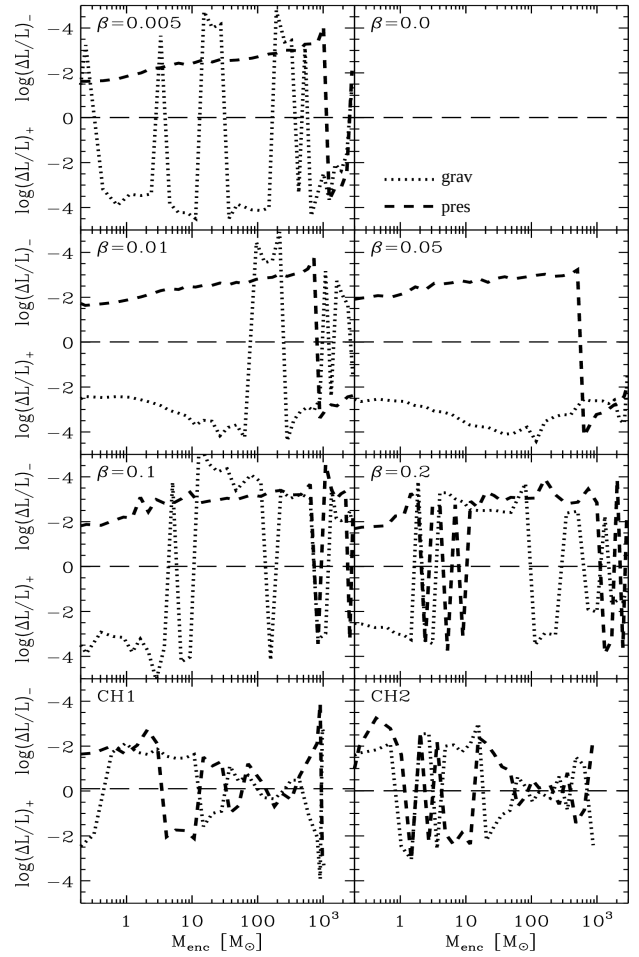


Fig. 3 The fractional change of the specific angular momentum ($\Delta L/L$) with the free-fall time of the mass shell due to the torques acting on the shell are plotted as a function of enclosed gas mass, just before formation of first protostar. The sign implies whether the angular momentum is gained (positive) or lost (negative) during collapse.

be more clear in terms of change of angular momentum that is shown in Fig. 3.

Taking the fractional change in the angular momentum of a shell ($\Delta L(r)/L(r)$) with the local free-fall time (t_{ff}), we find that both the torques are dominant throughout the evolution. As the collapse proceeds to higher densities, the angular momentum of a shell can increase or decrease depending on whether torques acting on the shell are positive or negative. We use $(\Delta L/L)_+$ and $(\Delta L/L)_-$ for the positive and negative fractional change of each type of torque (Fig. 3). The net change in the angular momentum happens due to the synchronous action of both the gravitational and pressure torque. However, in the inner regime, the cloud gains angular momentum due to the pressure gradient between the mass shell. On the other hand cloud's angular momentum is lost due to torque exerted by the gravity. This is consistent with the recent work by Greif et al. (2012) that concluded that the gravitational torque tends to decrease the angular momentum whereas the pressure torque does the opposite during the collapse of gas towards the protostellar densities. The spiral structure of the Keplerian disk that becomes gravitationally unstable can transfer the mass inside, thereby removing the extra angular momentum in the outward direction (Becerra et al. 2015). In addition, cosmological hydrodynamics simulations by Wise et al. (2008) has shown that the rotational secular bar instabilities can efficiently transport angular momentum outward in the central regime. It has also been suggested that for a simple hydrodynamical flow, the Reynolds stress associated with velocity fluctuations might act as a turbulent transport, and angular momentum can then be removed from the mean flow (Lodato 2008).

4 Summary and discussion

We have investigated in detail the angular momentum evolution during the collapse of the primordial gas and analysed its relation with other physical quantities. For this purpose, we have followed a systematic parameter study that spans two orders of magnitude in the strength of rotational support for the idealized solid body rotation along with two realistic cosmological minihalos.

We find that the initial configuration of the gas clouds (e.g. rotation, turbulence and halo-to-halo variation) have little influence on the distribution of the cloud's specific angular momentum. Apart from the

well-known density distribution, we find that the angular momentum **also provides** another way of explaining the properties of the primordial gas collapse. In addition, the sole dependency of the angular momentum on the gas mass makes it easier to understand the primordial star formation. These basic characteristics of the angular momentum distribution make it to be the fundamental property of the primordial gas collapse. We also discuss the possible mechanisms that are responsible for the power-law profile of angular momentum, mainly the simultaneous effect of the gravitational and pressure **torques**. We argue that the distribution is due to internal torques only and does not require the presence of turbulence or magnetic fields. However, the exact way of transferring the angular momentum, and **whether or not** it is related to the other physical properties, need further theoretical investigation.

The angular momentum distribution is an area of active research. There have been various investigations in a number of previous studies for the transport issues. For example, from the forefront studies by Larson (1969) to present theoretical studies (e.g., Yoshida et al. 2006; Bromm 2013; Hirano et al. 2015), people have tried to describe the plausible causes of the angular momentum transport especially for a system where magnetic fields have less or no contribution. The gravitational collapse of primordial gas is considered to be weakly magnetized (although recent simulations are showing the influence of the magnetic field, e.g., Sur et al. 2010). In such system, the pressure torque and gravitational torque could play an important role (although some studies consider only gravitational torque). We have performed a set of high-resolution simulations with varied rotation parameter (β_0) to study the angular momentum distribution. For the first time, to the best our knowledge, we have shown the effect of both the pressure torque as well as gravitational torque. Although our approach is different, we obtain similar results from previous forefront investigations (e.g., Yoshida et al. 2006; Greif et al. 2012). Our primary aim in this study was to investigate the distribution of the angular momentum, and we have shown how the distribution is related to the physical parameter of the collapsing gas. However, in describing the distribution along with the scaling relation, we have also made an attempt to discuss how the power-law behavior is controlled during the collapse. From our investigation, we can conclude that the distribution of angular momentum happens due to the concurrent effects of internal

torques in a collapsing system where turbulence or magnetic field does not play any significant role.

At this point, we would like to emphasize that we have discussed the possible source of transport only for a weakly magnetised Pop III collapse (Tan & McKee 2004; Bromm et al. 2009). On the other hand, the study by DeSouza & Opher (2008) has shown that the magnetic field plays an important role during collapse. The most common explanation for transfer of angular momentum is magnetized stellar winds and magnetic outflow (see e.g. Matt & Pudritz 2005). It has also been suggested that accretion disks threaded by a weak magnetic field are subject to magneto-hydrodynamics (MHD) instabilities (Balbus & Hawley 1998), which can induce turbulence in the disk, thereby being able to transport angular momentum and to promote the accretion process. However, in many astrophysical phenomena, such as the outer regions of protostellar disks, the ionization level is expected to be low, significantly reducing the effects of magnetic fields in determining the dynamics of the disk (Gammie 1996).

More recently the numerical simulations show the amplification of small seed fields up to dynamically important strengths during the collapse of primordial star-forming halos (Sur et al. 2010, 2012; Schleicher et al. 2010; Schober et al. 2012). The angular momentum can then be transported in the protostellar disk via magnetic braking (Machida & Doi 2013). However, the influence of the amplified magnetic fields on the redistribution of angular momentum requires further investigation.

The author acknowledges Prateek Sharma, Biman Nath and Kazu Omukai for the helpful comments on the manuscript. **The author also wish to thank the referee for constructive suggestions that have helped to improve the quality of the paper.** The author is grateful to the Centre for Theoretical Studies (CTS) of the Indian Institute of Technology–Kharagpur and the Department of Physics of the Indian Institute of Technology–Banaras Hindu University, Varanasi for the local hospitality. **The author would also like to thank the Inter-University Center for Astronomy and Astrophysics (IUCAA) at Pune for the local hospitality and financial support.** The present work is supported by the Indian Space Research Organization (ISRO) grant (No. ISRO/RES/2/367/10-11).

References

- Abel, T., Bryan, G. L., & Norman, M. L. 2000, *ApJ*, 540, 39
- Abel, T., Bryan, G. L., & Norman, M. L. 2002, *Science*, 295, 93
- Balbus, S. A., Hawley, J. F. 1998, *Rev. Mod. Phys.* 70, 1
- Bodenheimer, P. 1995, *ARA&A*, 33, 199B
- Bate M. R., Bonnell I. A., Bromm V. 2003. *MNRAS* 339, 577
- Barkana, R., Loeb, A., 2001, *Phys. Rep.*, 349, 125
- Becerra, F.; Greif, T. H.; Springel, V.; Hernquist, L. E, 2015, *MNRAS*, 446, 2380B
- Bromm, V., Coppi, P. S. & Larson, R. B., 1999, *ApJ*, 527L, 5B
- Bromm, V., Coppi, P. S., & Larson, R. B. 2002, *ApJ*, 564, 23
- Bromm, V., & Larson, R. B. 2004, *ARA&A*, 42, 79
- Bromm, V., Yoshida, N., Hernquist, L. & McKee, C. F. 2009, *Nature*, 459, 49
- Bromm, V., 2013, *RPPh*, 76k2901B
- Ciardi, B. & Ferrara A, 2005, *Space Sci. Rev.*, 116, 625
- Clark, P. C., Glover, S. C. O., Smith, R. J., Greif, T. H., Klessen, R. S. & Bromm, V. 2011, *Science*, 331, 1040
- Couchman, H. M. P., Rees, M. J., 1986, *MNRAS*, 221, 53C
- de Souza, R. S. & Opher, R., 2008, *PhRvD*, 77d, 3529D
- Dutta, J., 2015a, *ApJ*, 811, 98D
- Dutta, J., 2015b, Accepted for publication in the *A&A*, arXiv:1511.00285
- Dutta, J, Nath, B, B., Clark, P. C., Klessen, R. S., 2015, *MNRAS*, 450, 202D
- Dutta, J, Clark, P. C., Klessen, R. S., *AIP Conference Proceedings*, Vol 1480, pp. 333-336, 2012 (*POSTER PRIZE TALKS*)
- Fisher R. T. 2004, *Astrophys. J.* 600 76980
- Frebel, A., Aoki, W., Christlieb, N., Ando, H., Asplund, M., Barklem, P. S., Beers, T. C., Eriksson, K., Fechner, C., Fujimoto, M. Y., Honda, S., Kajino, T., Minezaki, T., Nomoto, K., Norris, J. E., Ryan, S. G., Takada-Hidai, M., Tsangarides, S., Yoshii, Y., 2005, *Natur*, 434, 871F
- Gammie, C. F., 1996, *ApJ*, 457, 355
- Glover, S. C. O. 2008, in *First Stars III, Chemistry and Cooling in Metal-Free and Metal-Poor Gas*, eds. B. O'Shea, A. Heger, (New York: AIP), 25, 990, 25G
- Glover, S. C. O., & Abel, T. 2008, *MNRAS*, 388, 1627
- Greif, T. H.; Bromm, V; Clark, P. C.; Glover, S. C. O.; Smith, R. J.; Klessen, R. S.; Yoshida, N.; Springel, V, 2012, *MNRAS*, 424, 399G
- Greif, T. H., 2015, *ComAC*, 2, 3G
- Haiman, Z.; Thoul, A. A.; Loeb, A, 1996, *ApJ*, 464, 523H
- Heger, A. & Woosley, S. E., 2002, *ApJ*, 567, 532H
- Hirano, S.; Hosokawa, T.; Yoshida, N.; Umeda, H.; Omukai, K.; Chiaki, G.; Yorke, H., 2014, *ApJ*, 781, 60H
- Hirano, S.; Hosokawa, T.; Yoshida, N.; Omukai, K.; Yorke, H., 2015, *MNRAS*, 448, 568H
- Hosokawa, T., Omukai, K., Yoshida Naoki & Yorke H. W. 2011, *Science*, 334, 1250
- Jappsen, A.-K.; Klessen, R. S., 2004, *A&A*, 423, 1J
- Johnson, J. L.; Dalla V. C.; Khochfar, S., 2013, *MNRAS*, 428, 1857J
- Latif, M. A.; Schleicher, D. R. G., 2015, *A&A*, 578A, 118L
- Lin Min-Kai, Krumholz M. R., Kratter K. M., 2011, *MNRAS*, 416, 580L
- Larson, R. B., 1969, *MNRAS*, 145, 271L
- Larson, R. B., 1972, *MNRAS*, 156, 437L
- Larson, R. B. 1984, *MNRAS*, 206, 197
- Lodato G., Rice W. K. M., 2004, *MNRAS*, 351, 630L
- Lodato G., 2008, *NewAR*, 52, 21L
- Matsumoto, T., Hanawa, T., Nakamura, F., 1997, *ApJ*, 478, 569
- Madao, P., 2000, *PhST*, 85, 156M, *Proceedings of Nobel Symposium* 109
- Machida, M. & Doi, K., 2013, *MNRAS*, 435, 3283M
- Norman, M. L.; Wilson, J. R.; Barton, R. T., 1980, *ApJ*, 239, 968N
- Matt, S., Pudritz, R. E. 2005 *MNRAS*, 356, 167
- Matt, S. P., Pinzn G., de la Reza R., Greene, T. P., 2010, *ApJ*, 714, 989
- Omukai, K., & Nishi, R. 1998, *ApJ*, 508, 141
- O'Shea, B. W., & Norman, M. L. 2007, *ApJ*, 654, 66
- O'Shea, B. W. & Norman, M. L., 2008, *ApJ*, 673, 14O
- Palla, F., Salpeter, E. E., & Stahler, S. W. 1983, *ApJ*, 271, 632
- Reed, D. S.; Bower, R.; Frenk, C. S.; Gao, L.; Jenkins, A.; Theuns, T.; White, Simon D. M., 2005, *MNRAS*, 363, 393R
- Silk, J., 1977, *ApJ*, 211, 638S
- Schneider, R.; Ferrara, A.; Salvaterra, R.; Omukai, K.; Bromm, V., 2003, *Nature*, 422, 869S
- Schober J., Schleicher D. R. G., Federrath C., Glover, S., Klessen R. S., Banerjee R. 2012, *ApJ*, 754, 99S
- Sur, S., Schleicher D. R. G., Banerjee R., Federrath C., & Klessen R. S. 2010, *ApJ*, 721, L134
- Sur, S., Federrath C., Schleicher D. R. G., Banerjee R., & Klessen R. S. 2012, *MNRAS*, 423, 3148S
- Schleicher, D. R. G., Banerjee, R., Sur, S., Arshakian, T. G., Klessen, R. S., Beck, R. & Spaans, M., 2010, *A&A*, 522, A115
- Springel, V., 2005, *MNRAS*, 364, 1105
- Springel, V., 2010, *MNRAS*, 401, 791S
- Sterzik, M. F., Durisen, H. & Zinnecker, H., 2003, *A&A*, 411, 91S
- Stacy, A., Bromm, V, & Loeb, A., 2011, *MNRAS* 413, 543
- Stacy, A. & Bromm, V., 2013, *MNRAS*, 433, 1094S
- Tan, J. C., & McKee C. F., 2004, *ApJ*, 603, 383
- Tegmark, M.; Silk, J.; Rees, M. J.; Blanchard, A.; Abel, T.; Palla, F., 1997, *ApJ*, 474, 1T
- Turk, M. J., Abel, T., & O'Shea, B. W. 2009, *Science*, 325, 601
- Umeda, H. & Nomoto, K., 2003, *Natur*, 422, 871U
- Vasiliev, E. O., Vorobyov, E. I., Shchekinov, Yu. A., 2010, *ARep*, 54, 890V
- Wise, J. H. & Abel, T., 2007, *ApJ*, 665, 899
- Wise, J. H.; Turk, M. J.; Abel, T., 2008, *ApJ*, 682, 745W
- Whalen, D., O'Shea, B. W., Smidt, J., Norman, M. L., 2008, *ApJ*, 679, 925W
- Yoshida, N., Omukai, K., Hernquist, L., & Abel, T. 2006, *ApJ*, 652
- Yoshida, N., Omukai, K., & Hernquist, L. 2008, *Science*, 321, 669